Phenomenological study of $\Omega_c \to \Omega^- \pi^+$ at polarized electron-positron collider

Yunlu Wang (王云路)[1†] Yunlong Xiao (肖云龙)[2‡] Pengcheng Hong (洪鹏程)[3,4§]

[1]College of Physics, Chengdu University of Technology, Chengdu 610059, China
[2]Key Laboratory of Nuclear Physics and Ion-beam Application (MOE) and Institute of Modern Physics, Fudan University, Shanghai 200433, China
[3]College of Physics, Jilin University, Changchun 130012, China
[4]Institute of High Energy Physics, the Chinese Academy of Sciences, Beijing 100049, China

Abstract: The exploration of symmetry laws stands as a cutting-edge direction in modern physics research. This study delves into the examination of P and CP symmetry properties within the charm quark system by analyzing asymmetry parameters in the two-body decay process of Ω_c. By accounting for the polarization effects of electron and positron beams and employing the helicity formalism, we systematically analyze the decay characteristics of Ω_c and its subsequent hyperon decays through specific asymmetry parameters. A comprehensive formulation of the angular distribution for these decay processes has been developed. The research assesses the detection sensitivity of asymmetry parameters in the $\Omega_c \to \Omega^- \pi^+$ decay mode across different experimental conditions, including varying data sample sizes and beam polarization configurations. These results contribute to enriching a theoretical foundation for forthcoming experimental endeavors at the STCF, offering significant implications for symmetry studies in the charm sector.

Keywords: beam polarization, symmetry, baryon, sensitivity

DOI: 10.1088/1674-1137/ae6311 **CSTR:** 32044.14.ChinesePhysicsC.50083101

I. INTRODUCTION

The observed matter-antimatter asymmetry of the universe remains one of the most compelling puzzles in modern physics. While the Big Bang should have produced equal amounts of matter and antimatter, cosmological observations unequivocally show a universe dominated by matter. This indicates that there must be a mechanism in the evolution of the universe that favors matter over antimatter. Charge parity (CP) violation is one of Sakharov's three essential conditions for understanding the matter and anti-matter asymmetry in the universe [1]. In the Standard Model of particle physics, the quark dynamics are described by the Cabibbo-Kobayashi-Maskawa (CKM) mechanism [2, 3]. This theoretical framework was experimentally confirmed through a series of landmark measurements. The BaBar and Belle collaborations reported the observation of indirect CP violation in the decay of B mesons [4, 5] in 2001. Subsequently, direct violation was observed during the rare decay process of B mesons [6, 7]. The first CP violation in the charm system was observed by the LHCb collaboration in 2019 [8]. Recent LHCb results have significantly expanded the experimental landscape, with evidence of CP violation in $\Lambda_b \to \Lambda K^+ K^-$ [9] and the first observation in $\Lambda_b \to p K^- \pi^+ \pi^-$ decays [10]. Similar searches of Λ, Σ^+, Ξ^0, and Ξ^- decays have also been performed by the BESIII collaboration [11−16]. However, all CP measurements are not sufficient to explain the differences between matter and antimatter. The search for new CP-violating mechanisms has thus become a central focus in particle physics, driving both theoretical innovations and next-generation experiments [17].

Theoretically, the decay amplitude of Ω_c consists of factorizable and non-factorizable contributions. While non-factorizable contributions are typically negligible in charmed meson decays, Ω_c decays exhibit unique dynamics, as their amplitudes can receive contributions from both W-emission and W-exchange diagrams. The W-exchange diagram (manifesting as a pole diagram) escapes helicity and color suppression, leading to non-trivial contributions. In the case of W-exchange processes, which can be represented as pole diagrams, the typical suppression mechanisms related to helicity and color no longer

Received 27 September 2025; Accepted 20 April 2026; Accepted manuscript online 21 April 2026
† E-mail: yunluwang20@fudan.edu.cn
‡ E-mail: xiaoyunlong@fudan.edu.cn (Corresponding author)
§ E-mail: hongpc@ihep.ac.cn

apply [18]. As a result, theoretical predictions for charmed baryon decays tend to be more complex compared to those for charmed mesons. Various theoretical frameworks have been developed to study these decays, such as the covariant confined quark model [19–21], the pole model [18, 22, 23], and current algebra [18, 23, 24]. The Cabibbo-favored decay $\Omega_c \to \Omega^-\pi^+$ is dominated by the W-emission process and also has a relatively large branching fraction, which makes it particularly interesting for studying parity (P) and CP violation. In Ω_c and $\bar{\Omega}_c$ two-body decays, the asymmetry parameters α_{Ω_c} and $\alpha_{\bar{\Omega}_c}$ quantify the contributions of P-wave (parity-violating) and D-wave (parity-conserving) amplitudes [25]. Specifically, α_{Ω_c} and $\alpha_{\bar{\Omega}_c}$ parameterize the decays of baryons and anti-baryons, where non-zero $\alpha_{\Omega_c}(\alpha_{\bar{\Omega}_c})$ and $(\alpha_{\Omega_c}+\alpha_{\bar{\Omega}_c})/(\alpha_{\Omega_c}-\alpha_{\bar{\Omega}_c})$ values mean P and CP violations. These features make Ω_c decays an ideal laboratory for symmetry test and polarization study, which can be explored at next-generation facilities. The Super Tau-Charm Facility (STCF) is designed to achieve a peak luminosity of 10^{35} cm^{-2}s^{-1} [26], representing a two-order-of-magnitude improvement over BESIII. With a center-of-mass energy range spanning $2-7$ GeV, which covers the production threshold for $\Omega_c\bar{\Omega}_c$ baryon pairs, STCF will enable unprecedented statistics for studies of charmed baryons. Recent theoretical studies have demonstrated that transverse and longitudinal beam polarization can improve parameter measurement precision at electron-positron colliders [27, 28].

In this paper, we present a systematic investigation of how beam polarization affects Ω_c polarization by comparing with polar and azimuthal angle distributions of particles from Ω_c decay. We report the first study of parameter sensitivity under different transverse and longitudinal polarization configurations. Furthermore, we evaluate the optimization effects of beam polarization schemes on CP violation. These phenomenological results establish crucial theoretical support to understand Ω_c decay at future STCF.

II. ANGULAR PARAMETERS

The decays in this analysis are described in a helicity formalism [29]. The helicity angles and amplitudes of the $\Omega_c\bar{\Omega}_c$ production and the decay of Ω_c are listed in Table 1, while the corresponding angles are shown in Fig. 1.

Table 1. Helicity angles and amplitudes in relative decays.

Decay	Helicity angle	Helicity amplitude
$\gamma^* \to \Omega_c(\lambda_1)\bar{\Omega}_c(\lambda_0)$	(θ_1,ϕ_1)	A_{λ_1,λ_0}
$\Omega_c(\lambda_1) \to \Omega^-(\lambda_2)\pi^+$	(θ_2,ϕ_2)	B_{λ_2}
$\Omega^-(\lambda_2) \to \Lambda(\lambda_3)K^-$	(θ_3,ϕ_3)	F_{λ_3}
$\Lambda(\lambda_3) \to p(\lambda_4)\pi^-$	(θ_4,ϕ_4)	H_{λ_4}

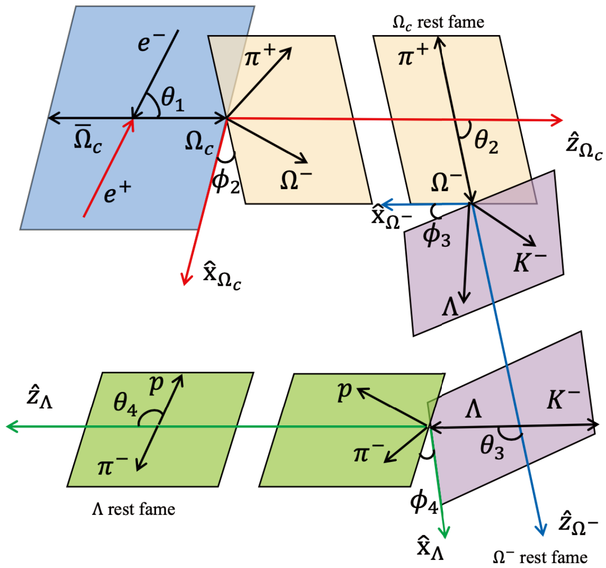

Fig. 1. (color online) Definition of helicity angles at e^+e^- collider.

The momenta p_i are obtained by boosting particle i to the rest frame of its mother particle, and the values of angles can be constructed by the momenta.

In general, a helicity amplitude for a two-body decay process can be denoted by $A^J_{\lambda_i,\lambda_j}$, where J denotes the spin of the mother particle and λ_i,λ_j are the helicity values of daughter particles, which are the projection of particle spin in momentum direction. Under parity conservation, the amplitudes will obey

$$A^J_{\lambda_i,\lambda_j} = \eta\eta_i\eta_j(-1)^{J-s_i-s_j}A^J_{-\lambda_i,-\lambda_j}, \tag{1}$$

where η_i is the intrinsic parity of each particle. The spins of the two daughter particles are denoted by s_i,s_j, respectively.

For the first process in Table 1, the helicity values can be $\lambda_1=\pm1/2$ and $\lambda_0=\pm1/2$ for spin-1/2 particles Ω_c and $\bar{\Omega}_c$. The photon has spin $J=1$ and parity $\eta=-1$, while the charmed baryons have $\eta_0=-1$, $\eta_1=1$ and $s_1=s_0=1/2$. For simplification, the superscript J is suppressed in the following such that $A_{\lambda_i,\lambda_j}=A^J_{\lambda_i,\lambda_j}$. The other amplitudes B,F and H listed in Table 1 follow a similar notation. We also suppress the subscripts corresponding to the daughter particles $\pi^\pm$ and K^- such as $B_{\lambda_2}=B_{\lambda_2,0}$, because they are spin-zero particles.

If all processes in Table 1 are parity conserved, the corresponding helicity amplitudes, A,B,F,H satisfy the following relations:

$$A_{\frac{1}{2},\frac{1}{2}} = A_{-\frac{1}{2},-\frac{1}{2}},\ A_{\frac{1}{2},-\frac{1}{2}} = A_{-\frac{1}{2},\frac{1}{2}},$$
$$B_{\frac{1}{2}} = B_{-\frac{1}{2}},\ F_{\frac{1}{2}} = F_{-\frac{1}{2}},\ H_{\frac{1}{2}} = -H_{-\frac{1}{2}}. \tag{2}$$

Here, the scripts are suppressed if they are fixed constants. Specifically, because of angular momentum conservation, only helicity values $\lambda_2 = \pm 1/2$ of Ω^- are allowed, which leads to two amplitudes $B_{\pm\frac{1}{2}}$. In the Standard Model, the P violations in weak decays make the above equations invalid. To quantify the violations, we define the following three asymmetric parameters:

$$\alpha_{\Omega_c} \equiv \frac{|B_{\frac{1}{2}}|^2 - |B_{-\frac{1}{2}}|^2}{|B_{\frac{1}{2}}|^2 + |B_{-\frac{1}{2}}|^2}, \tag{3}$$

$$\alpha_{\Omega^-} \equiv \frac{|F_{\frac{1}{2}}|^2 - |F_{-\frac{1}{2}}|^2}{|F_{\frac{1}{2}}|^2 + |F_{-\frac{1}{2}}|^2}, \tag{4}$$

$$\alpha_{\Lambda} \equiv \frac{|H_{\frac{1}{2}}|^2 - |H_{-\frac{1}{2}}|^2}{|H_{\frac{1}{2}}|^2 + |H_{-\frac{1}{2}}|^2}. \tag{5}$$

They are equivalent to original definitions from Lee-Yang [25] by decomposing amplitudes into S and P waves. The measured values of the last two parameters are $\alpha_{\Omega^-} = 0.0154 \pm 0.002$ [30] and $\alpha_\Lambda = 0.746 \pm 0.008$ [31], while the value of the parity parameter $\Omega_c \to \Omega^-\pi^+$ is still unknown.

Moreover, if CP conservation holds in charge conjugate decay $\bar{\Omega}_c \to \Omega^+\pi^-$, the parity parameter of this decay is expected to have the same absolute value but an opposite sign, that is, $\alpha_{\bar{\Omega}_c} = -\alpha_{\Omega_c}$. Thus, the CP violation can be characterized by

$$\mathcal{A}_{\rm CP} \equiv \frac{\alpha_{\Omega_c} + \alpha_{\bar{\Omega}_c}}{\alpha_{\Omega_c} - \alpha_{\bar{\Omega}_c}}. \tag{6}$$

This definition has the advantage that the systematic uncertainties of production and detection asymmetries are largely cancelled [32]. The approximation of the parameter can be expressed as [15, 33]

$$\mathcal{A}_{\rm CP} \propto -\tan\Delta\delta\tan\Delta\phi, \tag{7}$$

after inserting partial amplitudes. The relative strong phase $\Delta\delta$ predominantly arises from final-state interactions, which are discussed and computed within the QCD factorization framework [34, 35] and resonance-induced model [36] for B decays. The weak phase $\Delta\phi$ stems from interference between amplitudes with different partial wave configurations in the same decay [37]. The amplitudes partially derive from tree and penguin diagrams such as the examples shown in Fig. 2, where the tree diagram is Cabibbo-favored and the penguin diagram is suppressed from off-diagonal elements $V^*_{cb}V^*_{ts}$. The magnitude of the weak phase shift is determined by ${\rm Im}[-(V^*_{cb}V_{tb}V^*_{ts}V_{ud})]$ and expected at order of $O(10^{-4} \sim 10^{-5})$, which is close to predicted CP violation of hyperons systems [33, 38]. However, an additional suppression of order 10^{-5} arises from the extra Fermi constant $G_{\rm F}$ in the penguin diagram when the partial waves in Ref. [39] are incorporated. Consequently, the observable CP violation in Eq. (6) is subject to further suppression. Including the direct CP violation, a greater number cannot be ruled out for the mixing of strong violation and even new physics, which demands performing measurements at future e^+e^- collider.

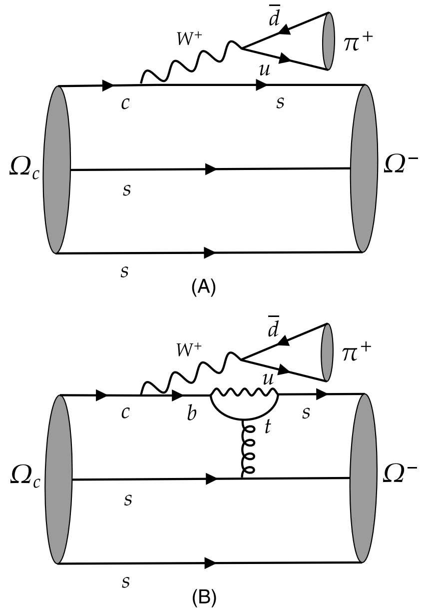

Fig. 2. Tree and penguin diagrams as examples for $\Omega_c \to \Omega^-\pi^+$ decay.

III. SPIN DENSITY MATRIX AND ANGULAR DISTRIBUTION

A. Ω_c production at e^+e^- collider

The density matrix (SDM) [40, 41] involves the spin and polarization information of particles. The SDM of spin-1/2 particles such as Ω_c is expressed by a 2×2 matrix:

$$\rho^{\Omega_c} = \frac{\mathcal{P}_0}{2}\begin{pmatrix} 1+P_z & P_x - {\rm i}P_y \\ P_x + {\rm i}P_y & 1-P_z \end{pmatrix}, \tag{8}$$

where $\mathcal{P}_0$ carries the unpolarized information, while the information of transverse polarization is taken by $\mathcal{P}_x$ and $\mathcal{P}_y$. Operator $\mathcal{P}_z$ represents longitudinal polarization. The information of initial collision is included by SDM of the virtual photon ρ^{γ^*}, which connects to ρ^{Ω_c} via the following equation:

$$\rho^{\Omega_c}_{\lambda_1,\lambda_1'} = \sum_{\lambda,\lambda_0} \rho^{\gamma^*}_{\lambda,\lambda'} D^{1*}_{\lambda,\lambda_1-\lambda_0}(\phi_1,\theta_1,0) \times D^{1}_{\lambda',\lambda_1'-\lambda_0}(\phi_1,\theta_1,0) A_{\lambda_1,\lambda_0} A^*_{\lambda_1',\lambda_0}, \tag{9}$$

where $D^J_{\lambda_j,\lambda_k}$ is the Wigner-D function. For polarized symmetric e^+e^- beams, when the transverse and longitudinal polarizations are considered simultaneously, the SDM of polarized photon is given by [28]

$$\rho^{\gamma^*}_{\lambda,\lambda'} = \frac{1}{2}\begin{pmatrix} (1-p_L)(1+\bar{p}_L) & 0 & p_T^2 \\ 0 & 0 & 0 \\ p_T^2 & 0 & (1+p_L)(1-\bar{p}_L) \end{pmatrix}. \tag{10}$$

In a positron-electron annihilation experiment with symmetric beam energy, the electron and positron share the same transverse polarization p_T respecting the z axis, which is chosen along the positron momentum shown in Fig. 1. The longitudinal polarizations of electrons is represented by factor p_L, and the ratio of the number of right-handed and left-handed electrons in the beam is determined by this factor through $(1+p_L)/(1-p_L)$, while factor $\bar{p}_L$ is for positrons. The diagonal elements indicate the fact that the photon couples either a single right-handed particle to a left-handed antiparticle or a single left-handed particle to a right- handed antiparticle.

We clarify the magnitude and phase angle of an amplitude by denoting $A_{\lambda_1,\lambda_0} = a_1 e^{i\zeta_1}$ and define the phase difference $\Delta_1 = \zeta_1 - \zeta_1'$. The other amplitudes take similar decompositions. Substituting Eq. (9) into Eq. (8) under parity conservation of Ω_c production, we obtain the unpolarized section, which depends on the polarizations of the virtual photon, that is

$$\mathcal{P}_0 = (1-p_L\bar{p}_L)(1+\alpha_c\cos^2\theta_1) + p_T^2\alpha_c\sin^2\theta_1\cos 2\phi_1. \tag{11}$$

Here, the constant $\frac{1}{2}|A_{\frac{1}{2},-\frac{1}{2}}|^2 + |A_{\frac{1}{2},\frac{1}{2}}|^2$ is suppressed because it does not contribute to the final cross sections after normalization. The angular distribution parameter α_c for this production is defined by

$$\alpha_c \equiv \frac{|A_{\frac{1}{2},-\frac{1}{2}}|^2 - 2|A_{\frac{1}{2},\frac{1}{2}}|^2}{|A_{\frac{1}{2},-\frac{1}{2}}|^2 + 2|A_{\frac{1}{2},\frac{1}{2}}|^2}, \tag{12}$$

which has not been measured yet. Next, given that the electromagnetic interaction is dominated for the production of the charged pair, we use hypothetical values $\alpha_c = 0.7$ and $\Delta_1 = \pi/6$, which are close to the measurements of strange baryons [42]. Our analysis framework is applicable to any value of α_c, and the actual value can be measured via the angular distribution of event number given in Eq. (20).

The transverse and longitudinal polarizations of Ω_c are

$$\mathcal{P}_x = \frac{\sqrt{1-\alpha_c^2}\sin\theta_1[(p_L-\bar{p}_L)\cos\Delta_1 - p_T^2\sin\Delta_1\sin 2\phi_1]}{1+\alpha_c\cos^2\theta_1 + p_T^2\alpha_c\sin^2\theta_1\cos 2\phi_1},$$

$$\mathcal{P}_y = \frac{\sqrt{1-\alpha_c^2}\sin\Delta_1\sin\theta_1\cos\theta_1(1-p_L\bar{p}_L - p_T^2\cos 2\phi_1)}{1+\alpha_c\cos^2\theta_1 + p_T^2\alpha_c\sin^2\theta_1\cos 2\phi_1},$$

$$\mathcal{P}_z = \frac{(1+\alpha_c)(\bar{p}_L-p_L)\cos\theta_1}{1+\alpha_c\cos^2\theta_1 + p_T^2\alpha_c\sin^2\theta_1\cos 2\phi_1}. \tag{13}$$

These polarizations reduce to the results in Ref. [28] when the incoming beams are polarized transversely, and turn to the expressions in Ref. [43] when the electron beam is polarized longitudinally. For continuity and simplicity, we also treat the longitudinal polarization of positron beam to be zero by setting $\bar{p}_L = 0$. We have found that the dependences of the results presented below on longitudinal beam polarizations are dominated by the difference $p_L - \bar{p}_L$. The $\cos\theta_1$ distribution of $\mathcal{P}_y$ can be obtained after integrating out ϕ_1, and its magnitude is improved by transverse polarization p_T, as plotted in Fig. 3. Because of the existence of polarized beams, the polarizations $\mathcal{P}_x$ and $\mathcal{P}_z$ are no longer flat; the $\cos\theta_1$ distribution of $\mathcal{P}_z$ is shown in Fig. 4. The distribution of magnitude $|\mathcal{P}_{\Omega_c}| = \sqrt{\mathcal{P}_x^2+\mathcal{P}_y^2+\mathcal{P}_z^2}$ is also represented in Fig. 5, highlighting discernible differences associated with different beam polarization configurations. The transverse polarization degree $P_T = 1$ is adopted for theoretical discussion, whereas in a realistic storage-ring environment, P_T is expected to be slightly less than unity owing to the Sokolov-Ternov effect [44].

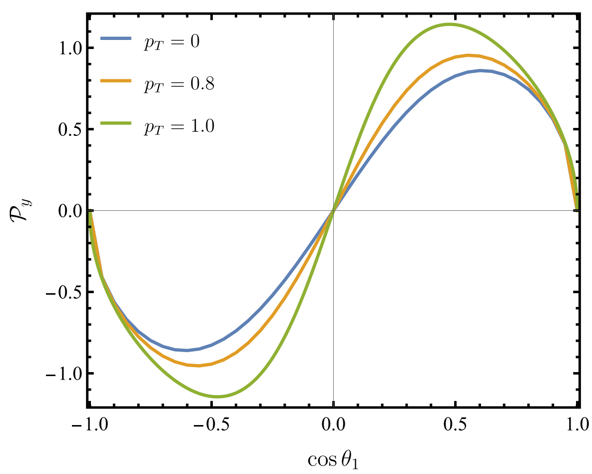

Fig. 3. (color online) Plots of $\cos\theta_1$ distributions of polarization $\mathcal{P}_y$ for different transverse polarizations of beams; here, we set $p_L = 0$.

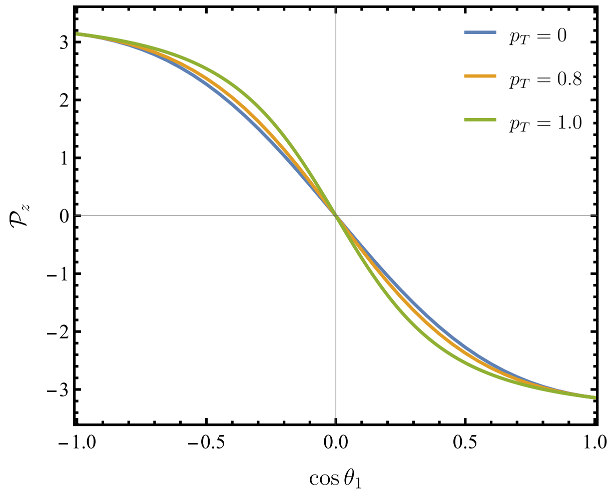

Fig. 4. (color online) Plots of $\cos\theta_1$ distributions of polarization $\mathcal{P}_z$ for different transverse polarizations of beams. Here, we set $p_L = 0.5$.

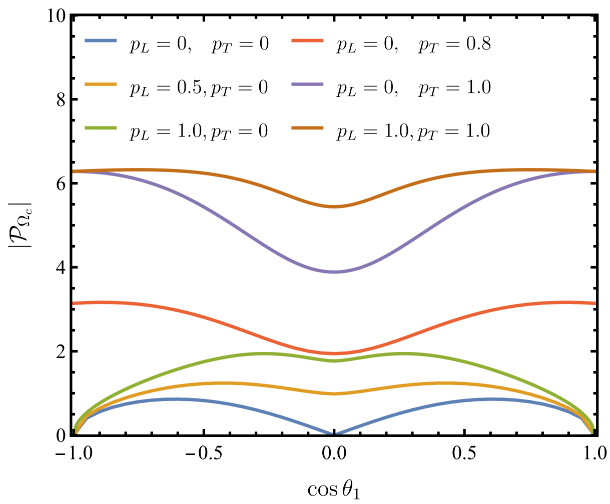

Fig. 5. (color online) Magnitudes of the Ω_c polarization as a function of $\cos\theta_1$ for different beam polarizations.

B. Two-body decays and joint angular distributions

The information of P violation of this two-body decay is carried by the SDM of Ω^-, which is given by the relation

$$\rho^{\Omega^-}_{\lambda_2,\lambda_2'} \propto \sum_{\lambda_1,\lambda_1'} \rho^{\Omega_c}_{\lambda_1,\lambda_1'} D^{\frac{1}{2}*}_{\lambda_1,\lambda_2}(\phi_2,\theta_2) D^{\frac{1}{2}}_{\lambda_1',\lambda_2'}(\phi_2,\theta_2) B_{\lambda_2} B_{\lambda_2'}, \tag{14}$$

where the helicity value λ_2 or λ_2' is either $1/2$ or $-1/2$, which means SDM ρ^{Ω^-} is also a 2×2 matrix such as those in Eq. (8). Then, after summing all combinations and implementing simplifications, the unpolarized and longitudinal-polarized operators of Ω^- reduce to

$$\mathcal{P}^{\Omega^-}_0 = \frac{2\mathcal{P}_0}{1+\alpha_{\Omega_c}} \left[1 + \alpha_{\Omega_c} \cos\theta_2 \mathcal{P}_z + \alpha_{\Omega_c} \sin\theta_2 \left(\cos\phi_2 \mathcal{P}_x + \sin\phi_2 \mathcal{P}_y\right)\right], \tag{15}$$

$$\mathcal{P}^{\Omega^-}_0 \mathcal{P}^{\Omega^-}_z = \frac{2\mathcal{P}_0}{1+\alpha_{\Omega_c}} \left\{\alpha_{\Omega_c} + \cos\theta_2 \mathcal{P}_z + \sin\theta_2 \left(\cos\phi_2 \mathcal{P}_x + \sin\phi_2 \mathcal{P}_y\right)\right\}, \tag{16}$$

and the transverse-polarized operators are

$$\mathcal{P}^{\Omega^-}_0 \mathcal{P}^{\Omega^-}_x = \mathcal{P}_0 \sqrt{\frac{1-\alpha_{\Omega_c}}{1+\alpha_{\Omega_c}}} \left\{\sin\Delta_2 \left(\mathcal{P}_y \cos\phi_2 - \mathcal{P}_x \sin\phi_2\right) - \cos\theta_2 \left[\mathcal{P}_z \sin\theta_2 - \left(\mathcal{P}_x \cos\phi_2 + \mathcal{P}_y \sin\phi_2\right)\right]\right\}, \tag{17}$$

$$\mathcal{P}^{\Omega^-}_0 \mathcal{P}^{\Omega^-}_y = \mathcal{P}_0 \sqrt{\frac{1-\alpha_{\Omega_c}}{1+\alpha_{\Omega_c}}} \left\{\cos\Delta_2 \left(\mathcal{P}_y \cos\phi_2 - \mathcal{P}_x \sin\phi_2\right) + \sin\theta_2 \left[\mathcal{P}_z \sin\theta_2 - \left(\mathcal{P}_x \cos\phi_2 + \mathcal{P}_y \sin\phi_2\right)\right]\right\}. \tag{18}$$

Finally, all parity information is compiled in the proton SDM, which is expressed by

$$\rho^{p}_{\lambda_4,\lambda_4'} \propto \sum_{\lambda_1,\lambda_1'} \rho^{\Omega_c}_{\lambda_1,\lambda_1'} B_{\lambda_2} B_{\lambda_2'} F_{\lambda_3} F_{\lambda_3'} H_{\lambda_4} H_{\lambda_4'} \times D^{\frac{1}{2}*}_{\lambda_1,\lambda_2}(\phi_2,\theta_2) D^{\frac{1}{2}*}_{\lambda_2,\lambda_3}(\phi_3,\theta_3) D^{\frac{1}{2}*}_{\lambda_3,\lambda_4}(\phi_4,\theta_4) \times D^{\frac{1}{2}}_{\lambda_1',\lambda_2'}(\phi_2,\theta_2) D^{\frac{1}{2}}_{\lambda_2',\lambda_3'}(\phi_3,\theta_3) D^{\frac{1}{2}}_{\lambda_3',\lambda_4'}(\phi_4,\theta_4). \tag{19}$$

The proton polarizations can be iteratively obtained using similar expressions to those of Eqs. (15)−(18); we suppress the explicit expressions here. The joint angular distribution is given by the unpolarized proton section $\mathcal{W} = \mathrm{Tr}\rho^p = \mathcal{P}^p_0$. The angular distribution of an event number N for each angle is obtained by integrating out other angles, and the nontrivial distributions are

$$\frac{\mathrm{d}N}{\mathrm{d}\cos\theta_1} \propto 1 + \alpha_c \cos^2\theta_1, \tag{20}$$

$$\frac{\mathrm{d}N}{\mathrm{d}\cos\theta_3} \propto 1 + \alpha_{\Omega_c}\alpha_{\Omega^-} \cos\theta_3, \tag{21}$$

$$\frac{\mathrm{d}N}{\mathrm{d}\cos\theta_4} \propto 1 + \alpha_{\Omega^-}\alpha_{\Lambda} \cos\theta_4, \tag{22}$$

$$\frac{\mathrm{d}N}{\mathrm{d}\phi_1} \propto 1 + \frac{\alpha_c}{3}\left(1 + 2p_T^2 \cos 2\phi_1\right), \tag{23}$$

$$\frac{\mathrm{d}N}{\mathrm{d}\phi_2} \propto 1+\frac{3\pi^2}{16}\alpha_{\Omega_c}\frac{\sqrt{1-\alpha_c^2}}{3+\alpha_c}p_L\cos\Delta_1\cos\phi_2\,, \tag{24}$$

$$\frac{\mathrm{d}N}{\mathrm{d}\phi_4} \propto 1-\frac{\pi^2}{16}\alpha_{\Omega_c}\alpha_\Lambda\sqrt{1-\alpha_{\Omega^-}^2}\cos(\Delta_3+\phi_4)\,. \tag{25}$$

The distributions of θ_2 and ϕ_3 are flat. The distributions in Eqs. (20) and (21) are used for fitting the values of parameters α_c and α_{Ω_c}. The distributions of ϕ_1, ϕ_2, and ϕ_4 are no longer flat when the beams are polarized transversely or longitudinally. The plot for the ϕ_1 distribution in Eq. (23) is shown in Fig. 6, where the fluctuation is not affected by the longitudinal polarization of the electron beam; it is enhanced by the transverse polarization, as shown in Fig. 7. Conversely, the ϕ_2 distribution is free of the value of p_T but depends on longitudinal polarization p_L.

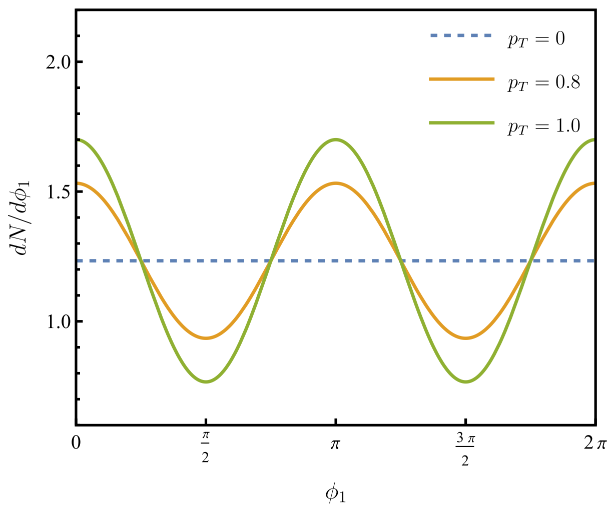

Fig. 6. (color online) Distributions of ϕ_1 for three different transverse beam polarizations.

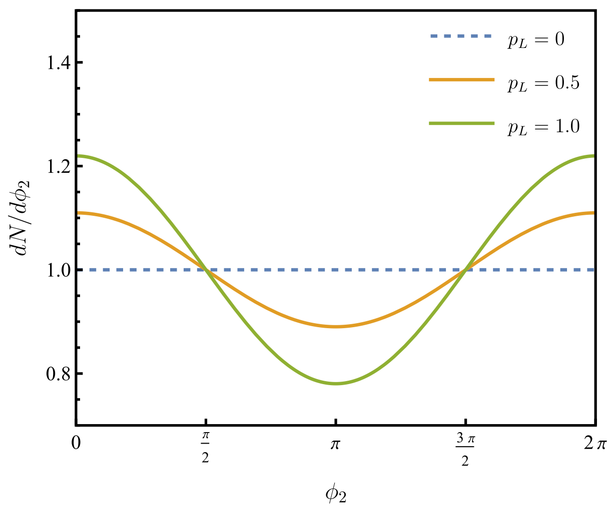

Fig. 7. (color online) Distributions of ϕ_2 for different longitudinal polarizations of electron beam. The normalization is arbitrary. Here, we set $\alpha_{\Omega_c} = 0.7$.

Theoretical predictions for the asymmetry parameter α_{Ω_c} are currently lacking. However, for the decays $\Xi_c^+ \to \Xi^0\pi^+$ and $\Xi_c^0 \to \Xi^-\pi^+$, which involve similar diagrams to those in Fig. 2 but with the spectator s quark replaced by a u or d quark, the absolute values of the corresponding asymmetry parameters are predicted to be around 0.95 and 0.7 [45–50], respectively. These values are used in the following analysis and should be verified at the STCF via Eq. (21). On the other hand, no measurement of the relevant parameter for $\Xi_c^+ \to \Xi^0\pi^+$ is currently available; it will be accessible at the future STCF.

The joint angular distributions of θ_1 and ϕ_1 are obtained by integrating out all angles of two-body decays, fulfilling the following expression:

$$\mathcal{W}(\theta_1,\phi_1) = -\frac{64\pi^3\mathcal{P}_0}{(1+\alpha_{\Omega_c})(1+\alpha_{\Omega^-})(1+\alpha_\Lambda)}\,. \tag{26}$$

Given that the unpolarized operator $\mathcal{P}_0$ in Eq. (11) depends on the beam polarization, the statistically measured polarization observables are also affected by the values of p_L and p_T. The measurements can be quantified by the weighted polarizations of Ω_c defined via

$$\langle\mathcal{P}_i\rangle = \int \mathcal{P}_i\mathcal{W}(\theta_1,\phi_1)\,\mathrm{d}\cos\theta_1\mathrm{d}\phi_1\,, \tag{27}$$

where $i\in\{0,x,y,z\}$. Explicitly, the expressions of the weighted distributions for $\cos\theta_1$ or ϕ_1 are

$$\frac{\mathrm{d}\langle\mathcal{P}_0\rangle}{\mathrm{d}\cos\theta_1} \propto 1+2\alpha_c\cos^2\theta_1+\alpha_c^2\left(\cos^4\theta_1+\frac{p_T^4}{2}\sin^4\theta_1\right), \tag{28}$$

$$\frac{\mathrm{d}\langle\mathcal{P}_x\rangle}{\mathrm{d}\cos\theta_1} \propto p_L\sin\theta_1\,, \tag{29}$$

$$\frac{\mathrm{d}\langle\mathcal{P}_z\rangle}{\mathrm{d}\cos\theta_1} \propto p_L\cos\theta_1\,, \tag{30}$$

$$\frac{\mathrm{d}\langle\mathcal{P}_y\rangle}{\mathrm{d}\cos\theta_1} \propto \sin\theta_1\cos\theta_1\,, \tag{31}$$

$$\frac{\mathrm{d}\langle\mathcal{P}_0\rangle}{\mathrm{d}\phi_1} \propto 1+\frac{2\alpha_c}{3}\left(1+2p_T^2\cos2\phi_1\right) + \frac{\alpha_c^2}{5}(1+2p_T^2\cos2\phi_1)^2\,, \tag{32}$$

$$\frac{\mathrm{d}\langle\mathcal{P}_x\rangle}{\mathrm{d}\phi_1} \propto p_L-p_T^2\tan\Delta_1\sin2\phi_1\,, \tag{33}$$

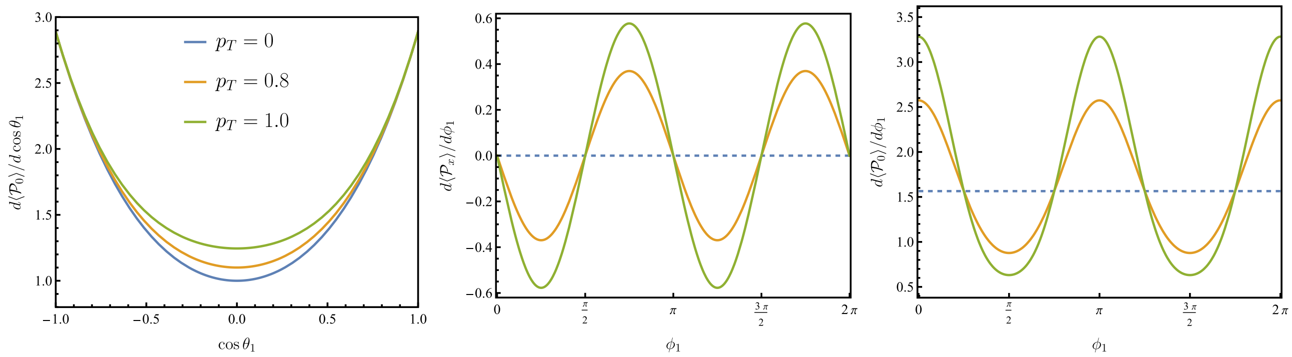

Fig. 8. (color online) Weighted polarizations of Ω_c as functions of ϕ_1 or θ_1 at different transverse beam polarizations. Here, we set $p_L = 0$.

where the factor p_L is retained for the distributions that have terms depending on p_L. Except for the $\cos\theta_1$ distribution of $\langle\mathcal{P}_0\rangle$ or $\langle\mathcal{P}_y\rangle$, other distributions are fluctuating only when the beams are polarized. The plots for Eqs. (28), (32), and (33) for different beam polarizations are shown in Fig. 8. The ϕ_1 distributions for weighted $\mathcal{P}_y$ and $\mathcal{P}_z$ are trivially zero. Furthermore, the values of p_L and Δ_1 can be determined by combining Eqs. (24) and (33) under fixed α_{Ω_c} and p_T.

IV. SENSITIVITY OF ASYMMETRIC PARAMETERS MEASUREMENTS

Sensitivity estimation is fundamental to experimental design, linking physical measurement precision to data statistics. We refine sensitivity estimation by using the entire decay chain for Ω_c. Our calculations show the expected precision for asymmetric parameters relative to data statistics. This method applies to similar decay processes. For large-scale facilities such as STCF [26], sensitivity estimation is urgently needed to guide the plan for data collection. Currently, the STCF detector and offline software system are in the research and development stage. Therefore, according to a design report [26], the reconstruction efficiency of this process is estimated to be 30%. We can discuss whether the facility could confirm or exclude certain theoretical scenarios after considering the impacts of the branching fractions and reconstruction efficiencies.

Our estimation is based on the maximum likelihood method. For the observed data sample of N events, the likelihood function is expressed as [51]

$$L(\theta_i,\phi_i,\alpha_c,\alpha_{\Omega_c},\alpha_{\Omega^-},\alpha_\Lambda) = \prod_{i=1}^{N} \widetilde{\mathcal{W}}_j, \tag{34}$$

where θ_i and ϕ_i represent polar angle and azimuth angle. The function depends on relative decay parameters $\alpha_c,\alpha_{\Omega_c},\alpha_{\Omega^-},\alpha_\Lambda$ and is computed based on the probability of the i-th event $\widetilde{\mathcal{W}}_j$, whose distribution is normalized. Then, the relative uncertainty for estimating statistical sensitivity to parity parameter α_{Ω_c} is defined as

$$\delta(\alpha_{\Omega_c}) = \frac{\sqrt{V(\alpha_{\Omega_c})}}{|\alpha_{\alpha_{\Omega_c}}|}, \tag{35}$$

where the inverse of the variance is given by

$$V^{-1}(\alpha_{\Omega_c}) = N\int \frac{1}{\widetilde{\mathcal{W}}}\left[\frac{\partial\widetilde{\mathcal{W}}}{\partial\alpha_{\Omega_c}}\right]^2 \prod_i^4 \mathrm{d}\cos\theta_i \mathrm{d}\phi_i, \tag{36}$$

where N denotes the number of observed events [51]. We consider a set of possible values of α_{Ω_c} to plot their sensitivities, shown in Fig. 9. At a fixed number of events, the statistical sensitivity is a monotonically decreasing function of the absolute value of the asymmetry parameter. The phases $\Delta_2 = \pi/4$ and $\Delta = \pi/3$ are employed here, and other sets of phase angle values do not significantly affect the statistical quantities.

We are particularly interested in the dependence of statistical sensitivities on asymmetry parameters and beam polarizations. The distributions of $\delta(\alpha_{\Omega_c})$ for four choices of the beam polarizations are plotted in Fig. 10 with α_{Ω_c} fixed at 0.7. The sensitivity improves as its value decreases by approximately 10% when the beam is

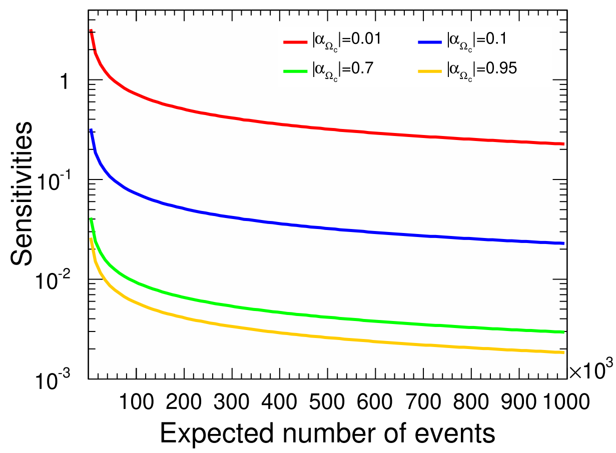

Fig. 9. (color online) Plots of the α_{Ω_c} sensitivity distributions relative to signal yields in terms of three different values.

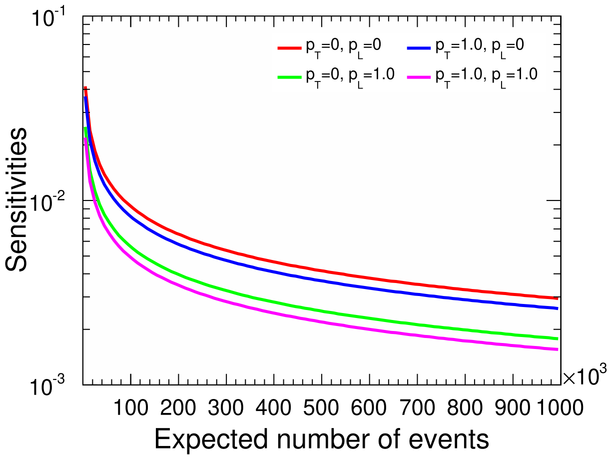

Fig. 10. (color online) Plots of the α_{Ω_c} sensitivity distributions relative to signal yields in terms of different beam polarizations.

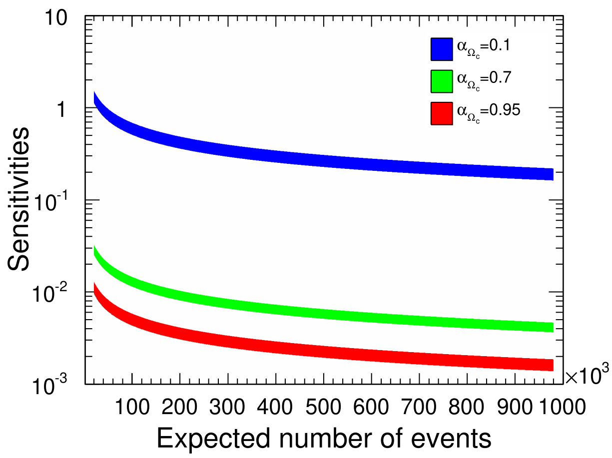

Fig. 11. (color online) Plots of $\mathcal{A}_{\rm CP}$ sensitivity distributions relative to signal yields in terms of two different values of α_{Ω_c}. The uncertainty from the CP parameter is $|\mathcal{A}_{\rm CP}| < 0.076$.

transversely polarized at $p_T = 1$ compared to an unpolarized scenario, and the value decreases by approximately 34% when the beam is longitudinally polarized at $p_L = 1$.

To identify the significance of CP violations, the statistical sensitivity of $\mathcal{A}_{\rm CP}$ in Eq. (6) can be estimated if α_{Ω_c} and $\bar{\alpha}_{\bar{\Omega}_c}$ are considered as non-correlation, via the following error propagation formula:

$$\delta(\mathcal{A}_{\rm CP}) = \frac{2\sqrt{\alpha^2_{\Omega_c}\delta(\bar{\alpha}_{\bar{\Omega}_c})^2 + \bar{\alpha}^2_{\bar{\Omega}_c}\delta(\alpha_{\Omega_c})^2}}{(\alpha_{\Omega_c} - \bar{\alpha}_{\bar{\Omega}_c})^2}, \tag{37}$$

where $\delta(\bar{\alpha}_{\bar{\Omega}_c})$ is the sensitivity for $\bar{\Omega}_c$ system. The plots for sensitivity $\delta(\mathcal{A}_{\rm CP})$ are shown in Fig. 11 for three different values of α_{Ω_c}. The sensitivity and CP parameter are positively correlated when other variables are fixed, and the bands are used to display uncertainty from variation $|\mathcal{A}_{\rm CP}| < 0.076$. Although the direct CP violation from weak interactions for decays of charm baryons is on the order of 10^{-4} or less, we adopt an upper limit of 0.076 according to prior experiments [52] to involve possible enhancements from other mechanisms. The value of $\mathcal{A}_{\rm CP}$ can be obtained by combining Eqs. (6) and (21), associated with determined $\alpha_{\bar{\Omega}_c}$ from the conjugation decay. The plots of $\delta(\mathcal{A}_{\rm CP})$ for four choices of the beam polarizations are shown in Fig. 12 with α_{Ω_c} fixed at 0.7. They exhibit similar line shapes and evolutionary trends as those in Fig. 10.

The expected number of observed signal events each year is estimated by assuming that the cross section of $e^+e^- \to \Omega_c\bar{\Omega}_c$ is approximately equal to that of $e^+e^- \to \Lambda_c^+\bar{\Lambda}_c^-$ [53, 54]. The branching fractions of intermediate processes and detection efficiency have been carefully considered in the calculations. The branching fraction of the $\Omega_c \to \Omega^-\pi^+$ decay was computed in Refs. [55–58]; a value of 4.2% [55] was chosen in our analysis. The

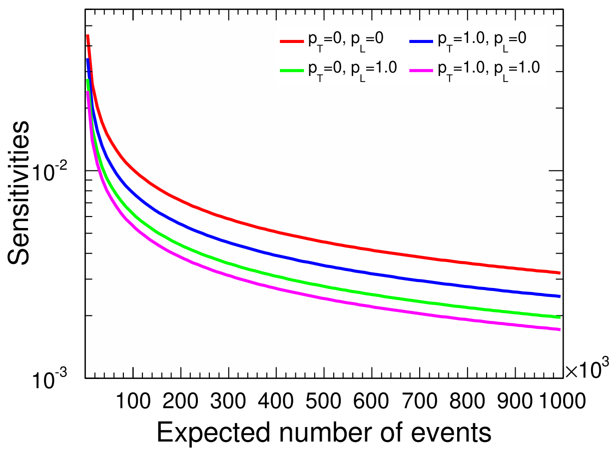

Fig. 12. (color online) Plots of the $\mathcal{A}_{\rm CP}$ sensitivity distributions relative to signal yields in terms of different beam polarizations.

Table 2. Statistical sensitivities $\delta_{\alpha_{\Omega_c}}$ and $\delta_{\mathcal{A}_{\rm CP}}$ for different parameter assumptions based on 0.37 million events expected. Here, we set $\mathcal{A}_{\rm CP}$ to 0.001.

Assumed parameters	$\delta_{\alpha_{\Omega_c}}$ (%)	$\delta_{\mathcal{A}_{\rm CP}}$ (%)
$\alpha_{\Omega_c} = 0.7$, $p_T = 0$, $p_L = 0$	0.48	0.49
$\alpha_{\Omega_c} = 0.95$, $p_T = 0$, $p_L = 0$	0.34	0.27
$\alpha_{\Omega_c} = 0.95$, $p_T = 1.0$, $p_L = 0$	0.28	0.22
$\alpha_{\Omega_c} = 0.95$, $p_T = 0$, $p_L = 1.0$	0.16	0.13
$\alpha_{\Omega_c} = 0.95$, $p_T = 1.0$, $p_L = 1.0$	0.14	0.10

branching fractions of $\Omega^- \to \Lambda K^+$ and $\Lambda \to p\pi^-$ were taken from Particle Data Group [59]. The detection efficiency of the signal channel was estimated to be 30%. Therefore, the observed $\Omega_c \to \Omega^-\pi^+ \to \Lambda K^+\pi^+ \to p\pi^- K^+\pi^+$ yields are expected to be ~ 0.37 million at STCF. Approximate values for α_{Ω_c}, inferred from the predicted parameters of Ξ_c^+ and Ξ_c^0 [51], can be tested at STCF with a precision of 0.48% and 0.34% for $|\alpha_{\Omega_c}| = 0.7$ and 0.95, respectively, as shown in Fig. 9. The expected CP violation in the $\Omega_c \to \Omega^-\pi^+$ decay from weak interactions is on the order of 10^{-9} to 10^{-10}. Therefore, it is estimated that at least 2.0×10^{18} $\Omega_c\bar{\Omega}_c$ events are required to observe CP violation, under the assumption of $\alpha_{\Omega_c} = 0.95$. We can achieve precise measurements of decay and CP parameters at STCF, but the data sample is not sufficient to observe CP violation unless some new physical contributions are made. The detailed statistical sensitivities $\delta(\alpha_{\Omega_c})$ and $\delta(\mathcal{A}_{\rm CP})$ for different parameter assumptions are listed in Table 2.

V. SUMMARY

The beam polarization can affect the transverse and longitudinal polarization distributions of Ω_c, as well as the angular distributions of θ_1 and ϕ_1 in the center-of-mass frame of the electron-positron system. By measuring the angular distribution of the Ω_c and particles from the Ω_c decay, we can infer the contributions of the transverse and longitudinal polarization of the electron-positron beam. Although both longitudinal and transverse beam polarizations can improve the precision of decay parameters and CP parameters, the longitudinal polarization exhibits greater sensitivity than the transverse polarization.

Currently, experiments have achieved preliminary control of beam polarization. For future studies, particularly in precision CP measurements, achieving controllable transverse and longitudinal polarization with high polarization ratio will be crucial. In this study, we evaluated the sensitivities of the asymmetry parameters and CP violation in the decay $\Omega_c \to \Omega^-\pi^+$ under various data sample sizes and beam polarization conditions. If the decay parameter itself is larger, the sensitivity will be higher, which means that an accurate result can be measured experimentally. The polarization-dependent angular distributions and sensitivity estimates developed in this study can be used to enhance the verification of various theoretical predictions for related decays such as $\Xi_c^+ \to \Xi^0\pi^+$ and $\Xi_c^0 \to \Xi^-\pi^+$ at the STCF. This study represents the first investigation of P and CP violation in the two-body decay of Ω_c, providing essential theoretical support for future experiments, such as STCF.

References

[1] A. D. Sakharov, Pisma Zh. Eksp. Teor. Fiz. **5**, 32 (1967)
[2] N. Cabibbo, Phys. Rev. Lett. **10**, 531 (1963)
[3] M. Kobayashi and T. Maskawa, Prog. Theor. Phys. **49**, 652 (1973)
[4] A. Abashian *et al.* (Belle Collaboration), Phys. Rev. Lett. **86**, 2509 (2001)
[5] B. Aubert *et al.* (BaBar Collaboration), Phys. Rev. Lett. **86**, 2515 (2001)
[6] Y. Chao *et al.* (Belle Collaboration), Phys. Rev. Lett. **93**, 191802 (2004)
[7] B. Aubert *et al.* (BaBar Collaboration), Phys. Rev. Lett. **93**, 131801 (2004)
[8] R. Aaij *et al.* (LHCb Collaboration), Phys. Rev. Lett. **122**(21), 211803 (2019)
[9] R. Aaij *et al.* (LHCb Collaboration), Phys. Rev. Lett. **134**, 101802 (2025)
[10] R. Aaij *et al.* (LHCb Collaboration), Nature **643**, 1223 (2025)
[11] M. Ablikim *et al.* (BESIII Collaboration), Phys. Rev. Lett. **129**(13), 131801 (2022)
[12] M. Ablikim *et al.* (BESIII Collaboration), Phys. Rev. Lett. **131**(19), 191802 (2023)
[13] M. Ablikim *et al.* (BESIII Collaboration), Phys. Rev. Lett. **135**(14), 141804 (2025)
[14] M. Ablikim *et al.* (BESIII Collaboration), Phys. Rev. D **108**(3), L031106 (2023)
[15] M. Ablikim *et al.* (BESIII Collaboration), Nature **606**(7912), 64 (2022)
[16] M. Ablikim *et al.* (BESIII Collaboration), Phys. Rev. Lett. **132**(10), 101801 (2024)
[17] X. G. He, J. Tandean, and G. Valencia, Sci. Bull. **67**, 1840 (2022)
[18] H. Y. Cheng and B. Tseng, Phys. Rev. D **48**, 4188 (1993)
[19] J. G. Körner, G. Kramer, and J. Willrodt, Phys. Lett. B **78**, 492 (1978)
[20] J. G. Korner and M. Kramer, Z. Phys. C **55**, 659 (1992)
[21] M. A. Ivanov, J. G. Korner, V. E. Lyubovitskij *et al.*, Phys. Rev. D **57**, 5632 (1998)
[22] H. Y. Cheng and B. Tseng, Phys. Rev. D **46**, 1042 (1992)
[23] K. K. Sharma and R. C. Verma, Eur. Phys. J. C **7**, 217 (1999)
[24] T. Uppal, R. C. Verma, and M. P. Khanna, Phys. Rev. D **49**, 3417 (1994)
[25] T. D. Lee and C. N. Yang, Phys. Rev. **108**, 1645 (1957)
[26] M. Achasov *et al.*, Front. Phys. (Beijing) **19**(1), 14701 (2024)
[27] S. Zeng, Y. Xu, X. R. Zhou *et al.*, Chin. Phys. C **47**(11), 113001 (2023)
[28] X. Cao, Y. T. Liang, and R. G. Ping, Phys. Rev. D **110**, 014035 (2024)
[29] S. U. Chung, (1971), 10.5170/CERN-1971-008.
[30] Y. C. Chen *et al.* (HyperCP Collaboration), Phys. Rev. D **71**, 051102 (2005)
[31] M. Ablikim *et al.* (BESIII Collaboration), Phys. Rev. Lett. **133**(10), 101902 (2024)
[32] J. P. Wang and F. S. Yu, Phys. Lett. B **849**, 138460 (2024)
[33] J. F. Donoghue, X. G. He, and S. Pakvasa, Phys. Rev. D **34**, 833 (1986)
[34] M. Beneke, G. Buchalla, M. Neubert *et al.*, Nucl. Phys. B **591**, 313 (2000)
[35] M. Beneke, G. Buchalla, M. Neubert *et al.*, Nucl. Phys. B **606**, 245 (2001)

[36] H. Y. Cheng, C. K. Chua, and A. Soni, Phys. Rev. D **71**, 014030 (2005)
[37] M. Saur and F. S. Yu, Sci. Bull. **65**, 1428 (2020)
[38] J. Tandean and G. Valencia, Phys. Rev. D **67**, 056001 (2003)
[39] J. P. Wang, Q. Qin, and F. S. Yu, arXiv: 2411.18323 [hep-ph]
[40] M. G. Doncel, P. Mery, L. Michel *et al*., Phys. Rev. D **7**, 815 (1973)
[41] H. Chen and R. G. Ping, Phys. Rev. D **102**, 016021 (2020)
[42] M. Ablikim *et al*. (BESIII Collaboration), Phys. Lett. B **770**, 217 (2017)
[43] N. Salone, P. Adlarson, V. Batozskaya *et al*., Phys. Rev. D **105**(11), 116022 (2022)
[44] A. A. Sokolov and I. M. Ternov, Dokl. Akad. Nauk SSSR **153**(5), 1052 (1963)
[45] P. Zenczykowski, Phys. Rev. D **50**, 5787 (1994)
[46] Z. P. Xing, X. G. He, F. Huang *et al*., Phys. Rev. D **108**(5), 053004 (2023)
[47] H. Zhong, F. Xu, Q. Wen *et al*., JHEP **02**, 235 (2023)
[48] Z. P. Xing, Y. J. Shi, J. Sun *et al*., Eur. Phys. J. C **84**(10), 1014 (2024)
[49] H. Zhong, F. Xu, and H. Y. Cheng, Phys. Rev. D **109**(11), 114027 (2024)
[50] P. Y. Niu, Q. Wang, and Q. Zhao, Phys. Rev. D **111**(9), 093004 (2025)
[51] T. Z. Han, R. G. Ping, T. Luo *et al*., Chin. Phys. C **44**, 013002 (2020)
[52] Y. B. Li *et al*. (Belle Collaboration), Phys. Rev. Lett. **127**(12), 121803 (2021)
[53] M. Ablikim *et al*. (BESIII Collaboration), Phys. Rev. Lett. **131**(19), 191901 (2023)
[54] M. Ablikim *et al*. (BESIII Collaboration), Phys. Rev. D **109**(5), 053005 (2024)
[55] H. Y. Cheng, Phys. Rev. D **56**, 2799 (1997)
[56] Y. K. Hsiao, L. Yang, C. C. Lih *et al*., Eur. Phys. J. C **80**(11), 1066 (2020)
[57] K. L. Wang, Q. F. Lü, J. J. Xie *et al*., Phys. Rev. D **107**(3), 034015 (2023)
[58] S. Zeng, F. Xu, and Y. Gu, Eur. Phys. J. C **85**(2), 184 (2025)
[59] S. Navas *et al*. (Particle Data Group), Phys. Rev. D **110**(3), 030001 (2024)